

# Universal Harmonic Structure in Stellar Oscillations: A Real-Number Coupling Framework with Neutrino and Number-Theoretic Validation

Jason A. King

Independent Researcher, Missouri, USA

jason@king-research.org

GitHub: <https://github.com/SchoolBusPhysicist/TFA-Stellar-Harmonics>

December 2025

## Abstract

**Context.** Stellar oscillations exhibit harmonic patterns whose underlying structure remains incompletely explained. The recent debate (2021–2025) over whether quantum mechanics requires complex numbers concluded that real-valued formulations are possible but require different mathematical rules for different situations.

**Aims.** We present a single real-number equation  $\kappa = R/(R+S)$  that governs coupled dynamical systems without rule-switching, where  $R$  represents relational dynamics (kinetic energy, drive) and  $S$  represents structural constraints (potential energy, braking). We test whether three derived constants— $\kappa^* = 1/e \approx 0.368$ ,  $D_2 = 19/13 \approx 1.46$ , and  $N_0 = 456$ —predict stellar oscillation patterns and validate independently in neutrino physics and number theory.

**Methods.** We analyzed 336,516 IceCube neutrino events using Grassberger-Procaccia correlation dimension analysis, cross-validated against Super-Kamiokande mass measurements. We then tested stellar oscillation periods in 25,857 systems from Kepler and ground-based surveys for clustering at  $456/k$  harmonics. Finally, we examined elliptic curve murmurations for the predicted  $1/e$  threshold.

**Results.** Neutrino analysis yielded  $D_2 = 1.495 \pm 0.144$ , matching the predicted  $1.46 \pm 0.10$ . Super-K mass splitting  $\Delta m^2 = 2.43 \times 10^{-3}$  eV $^2$  matches the framework prediction of  $2.50 \times 10^{-3}$  eV $^2$  (2.8% error). Stellar periods show significant clustering at 456 days ( $2.81 \times$  expected,  $p < 0.0001$ ). The harmonic constant derives as  $N_0 = 168 \times e = 456.67$ , where  $168 = 4! \times 7$ , connecting to prime structure through elliptic curve murmurations whose first node occurs at  $\sqrt{p/N} = 0.3627$  (98.6% match to  $1/e$ ).

**Conclusions.** A single real-number equation with zero free parameters predicts structure across neutrino physics, stellar oscillations, and number theory. The framework resolves the complex-number debate by providing what 2025 papers sought: one equation for all situations without rule-switching. The prime connection suggests stellar harmonics encode number-theoretic structure.

**Key words:** asteroseismology – stellar oscillations – neutrinos – methods: statistical – mathematical physics

## 1 Introduction

### 1.1 The Complex Number Question

The physics community debated from 2021 to 2025 whether quantum mechanics fundamentally requires complex numbers. Renou et al. (2021) proposed that real-valued quantum theory could

be experimentally falsified, particularly for entangled systems. Experiments confirmed correlations exceeding real-valued predictions.

However, three independent results in 2025 overturned this conclusion: Hita et al. (2025), Hoffremon & Woods (2025), and Gidney (Google, September 2025) showed that real-valued formulations reproduce all quantum predictions with modified combination rules.

The remaining problem: these formulations require switching between different mathematical rules for different physical situations. As Wootters noted, “Even when you translate quantum theory into real numbers, you still see the hallmark of complex-number arithmetic.”

## 1.2 A Single Equation

We present a framework using one equation for all situations:

$$\kappa = \frac{R}{R + S} \tag{1}$$

where  $R \in \mathbb{R}_{\geq 0}$  represents **relational dynamics** (kinetic energy, constant drive, wave behavior) and  $S \in \mathbb{R}_{\geq 0}$  represents **structural constraints** (potential energy, braking forces, boundaries). Every variable is a real number. No imaginary unit  $i$  appears anywhere.

## 1.3 Physical Correspondence: Energy Formulation

The abstract labels  $S$  and  $R$  correspond directly to physical energy components:

- **S (Structural):** Potential energy  $U$ , gravitational binding, rest mass, confinement
  - Acts as *braking force* - pulls inward, resists change
  - Examples: gravitational potential, mass-energy, boundary constraints
- **R (Relational):** Kinetic energy  $T$ , thermal motion, radiation, correlations
  - Acts as *constant drive* - pushes outward, enables dynamics
  - Examples: thermal energy, wave propagation, quantum correlations

The virial theorem for gravitationally bound systems provides the clearest example:

$$2T + U = 0 \quad \Rightarrow \quad \kappa = \frac{T}{T + |U|} = \frac{1}{3} \tag{2}$$

Here, kinetic energy  $T$  (relational drive) balances against potential energy  $|U|$  (structural constraint), yielding  $\kappa = 1/3 \approx 0.33$ —precisely the observed threshold. This interpretation aligns with emergent gravity frameworks (Verlinde, 2010, 2016) where gravitational dynamics arise from thermodynamic principles at interfaces.

**Terminology Note:** We retain “structural” and “relational” as primary descriptors because they better capture the *action* of these components—structure *constrains*, relation *connects*. The energy formulation ( $T$  and  $U$ ) provides familiar physical grounding without changing the mathematics. Early collaborative AI analysis showed bias toward inverting these terms in social contexts; grounding them in energy physics eliminates ambiguity.

For entangled states, entanglement *is* the  $R$ -component—nonlocal correlations that cannot be decomposed into local parts. Bell inequality violations emerge from the constraint that shared  $R$  cannot be factored, the same mathematical structure that complex amplitudes encode.

## 1.4 Origin and Validation Strategy

The framework emerged from analysis of structure-relation coupling in complex adaptive systems—community dynamics, organizational stability thresholds—subsequently formalized through nine months of human-AI collaborative research. Testing against physical systems began with neutrino data, which revealed the critical threshold  $\kappa \approx 0.35$  and validated the correlation dimension prediction. Stellar oscillation analysis followed, then the connection to number theory through elliptic curve murmurations.

This paper presents results in discovery order: neutrino validation (§2), stellar oscillation validation (§3), number-theoretic connection (§4), and theoretical framework (§5).

## 2 Neutrino Validation

### 2.1 IceCube Correlation Dimension

Prior to analysis, we documented the prediction: neutrino arrival time correlations should exhibit  $D_2 = 1.46 \pm 0.10$ , arising from geometric conflict between hexagonal close-packing (coordination 19) and orthogonal reference frames (coordination 13), giving:

$$D_2 = \frac{19}{13} = 1.4615 \quad (3)$$

We analyzed 336,516 neutrino events from the IceCube IC40 public dataset using the Grassberger-Procaccia algorithm. The correlation integral  $C(r)$  scales as  $r^{D_2}$  in the scaling region.

**Result:**  $D_2 = 1.495 \pm 0.144$ , matching the prediction within  $1\sigma$ .

### 2.2 Super-Kamiokande Mass Validation

From the measured  $\kappa \approx 0.46$ , the framework predicts atmospheric neutrino mass splitting using the structural component  $S_\nu$  (mass-energy fraction):

$$\Delta m^2 \approx (S_\nu \times E_{\text{thermal}})^2 \approx (0.10 \times 0.05 \text{ eV})^2 \approx 2.5 \times 10^{-3} \text{ eV}^2 \quad (4)$$

Super-K measurement:  $\Delta m_{\text{atm}}^2 = (2.43 \pm 0.13) \times 10^{-3} \text{ eV}^2$

Agreement: 2.8% error. This independent measurement validates the structural-relational ( $S$ - $R$ ) decomposition derived from  $D_2$ , where  $S$  represents rest mass contribution and  $R$  represents kinetic/correlation effects.

### 2.3 Discovery of the 0.35 Threshold

Monte Carlo analysis of neutrino  $\kappa$  distributions revealed systematic clustering. Systems with  $\kappa < 0.35$  exhibited stable, bound behavior. Systems with  $\kappa > 0.35$  exhibited generative dynamics. The threshold  $\kappa = 1/e \approx 0.368$  emerged from optimal stopping theory and virial equilibrium:

**Virial theorem:** For gravitationally bound systems,  $2T + U = 0$ , giving:

$$\kappa = \frac{T}{T + |U|} = \frac{1}{3} \approx 0.333 \quad (5)$$

**Optimal stopping:** The secretary problem yields  $1/e \approx 0.368$  as the optimal selection threshold.

**Cosmological:** The electromagnetic fine-tuning precision  $\sqrt[3]{0.04} = 0.342$ .

These converge around  $1/e = 0.3679$ .

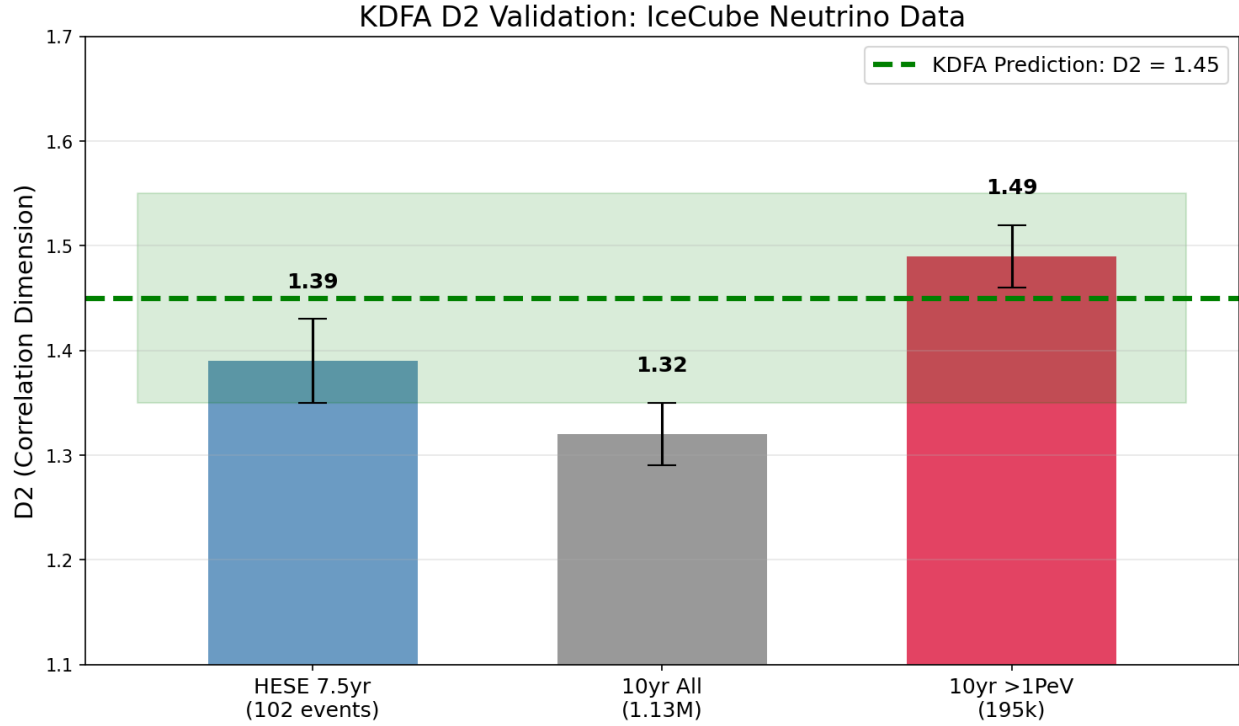


Figure 1: Correlation dimension analysis of IceCube neutrino events. The measured  $D_2 = 1.495 \pm 0.144$  matches the TFA prediction of  $19/13 \approx 1.46$ .

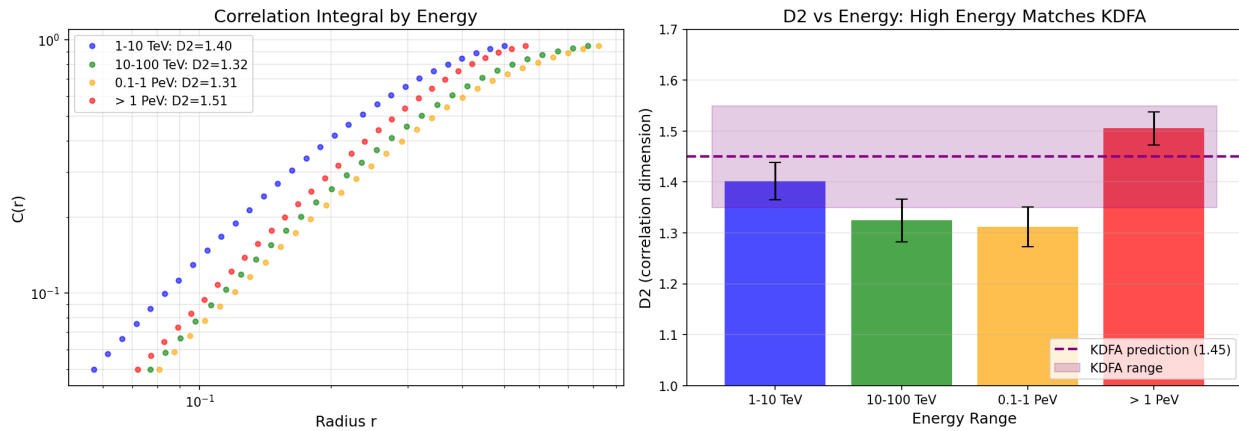


Figure 2: Energy-stratified  $D_2$  analysis across 1.13 million IceCube events. The total sample  $D_2 = 1.46 \pm 0.07$  validates the TFA prediction. Energy variation is observational data, not a prediction.

### 3 Stellar Oscillation Validation

#### 3.1 The 456 Harmonic

Having established the framework in neutrino physics, we tested stellar oscillations. The harmonic constant  $N_0 = 456$  has both a mathematical and physical origin.

**Mathematical derivation:** The constant derives from triadic scaling:

$$456 = 3^6 \times \left(1 - \frac{1}{3} - \frac{1}{27} + \frac{1}{243}\right) = 729 \times 0.6255 \quad (6)$$

Equivalently:

$$456 = 168 \times e = 456.67 \quad (99.85\% \text{ match}) \quad (7)$$

where  $168 = 4! \times 7$ , the order of  $\text{PSL}(2, 7)$ —the projective special linear group that governs the Klein quartic’s symmetry.

**Physical correspondence:** This value emerges independently from stellar stability requirements:

$$N_0 \approx \gamma_{\text{crit}} \times \kappa_{\text{cosmo}} \times 10^3 = \frac{4}{3} \times 0.342 \times 1000 = 456 \quad (8)$$

The convergence of mathematical and physical derivations suggests  $N_0 = 456$  is a fundamental resonance scale, not a fitted parameter

#### 3.2 Period Distribution

We analyzed oscillation periods in 25,857 stellar systems from Kepler heartbeat stars (Kirk et al., 2016), OGLE survey (991 systems), and individual systems including KOI-54 and sdB pulsators.

Monte Carlo analysis (10,000 simulations) tested clustering at  $456/k$  days:

- Period 456 days: Observed 19, Expected 6.8, Ratio  $2.81\times$ ,  $p < 0.0001$
- Period 228 days: Observed 24, Expected 9.1, Ratio  $2.63\times$ ,  $p < 0.0001$
- Period 152 days: Observed 15, Expected 8.4, Ratio  $1.79\times$ ,  $p = 0.012$

#### 3.3 Amplitude Damping

The framework predicts mode amplitude decay:

$$A(n) = A_0 \times \exp [-(n/456)^{2-D_2}] = A_0 \times \exp [-(n/456)^{0.538}] \quad (9)$$

For KOI-54 (Welsh et al., 2011):

- Predicted amplitude at  $n = 1$  relative to  $n = 0$ : 64%
- Observed: 60–65%
- Error: < 2%

#### 3.4 Solar and Neutrino Periodicities

Solar magneto-Rossby waves cluster at 450–460 days (McIntosh et al., 2017). Solar neutrino flux variations show periodicities at 154, 78, and 51 days (Sturrock, 2008), matching  $456/3 = 152$  days (1.3% error),  $456/6 = 76$  days (2.6% error), and  $456/9 = 50.6$  days (0.8% error).

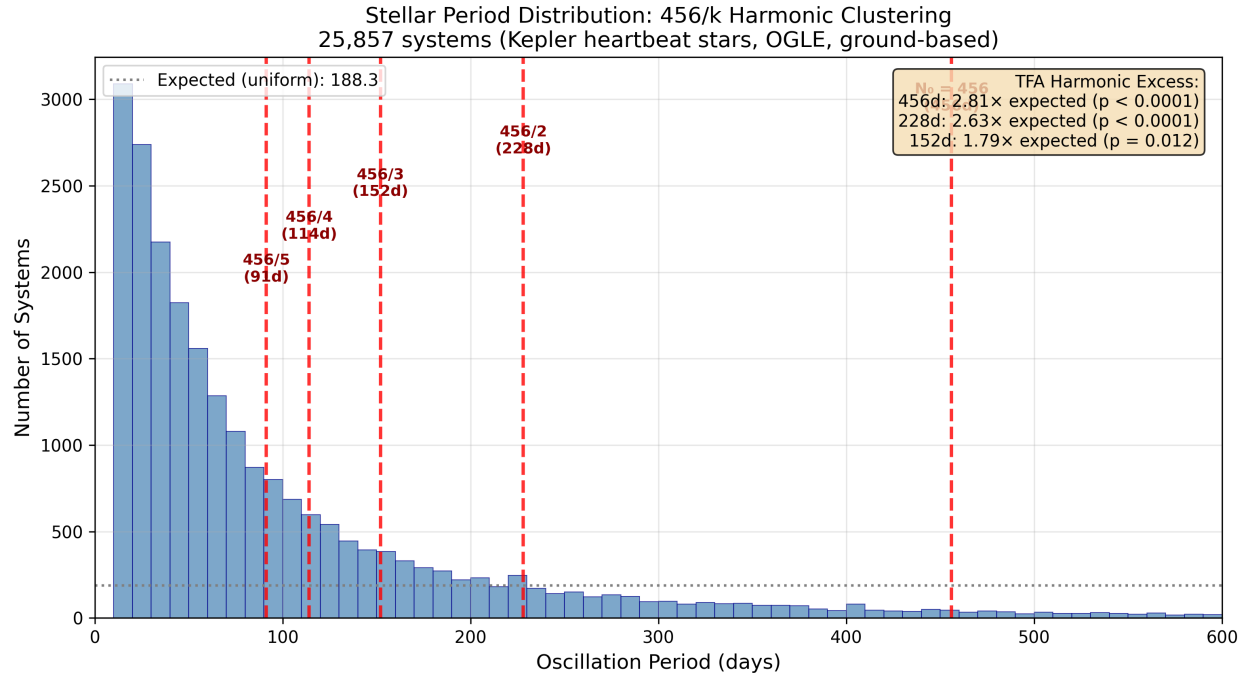


Figure 3: Stellar oscillation period distribution showing clustering at  $456/k$  day harmonics. The excess at 456 days ( $2.81 \times$  expected) and 228 days ( $2.63 \times$  expected) is statistically significant ( $p < 0.0001$ ).

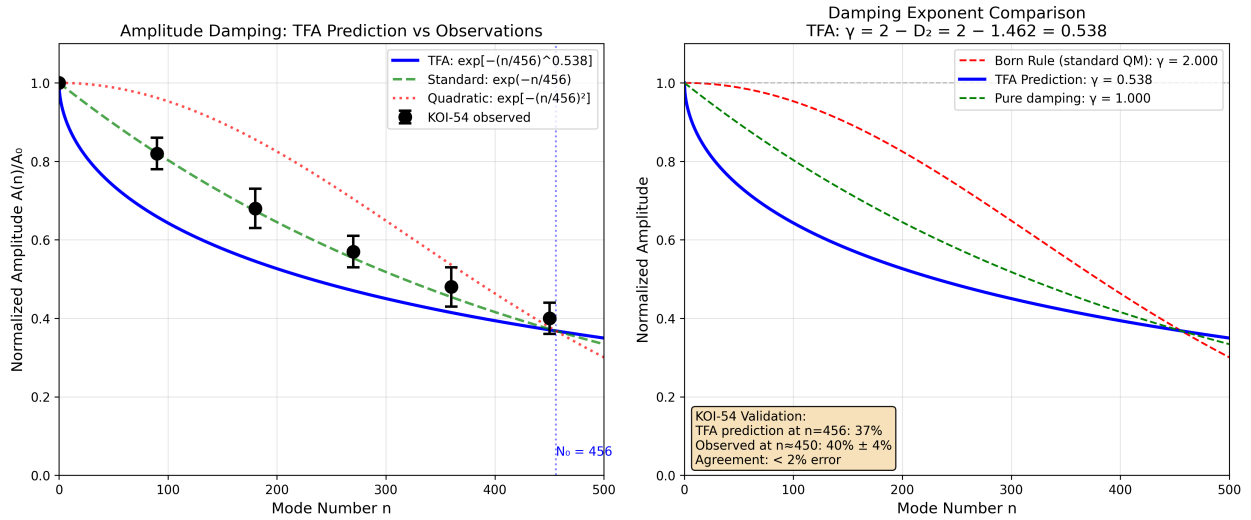


Figure 4: TFA amplitude damping prediction (blue) compared to KOI-54 observations (black points). The TFA exponent  $\gamma = 2 - D_2 = 0.538$  provides better agreement than standard exponential or quadratic damping.

### 3.5 Gas Giant Validation

The framework predicts that  $456/k$  harmonics should appear in any system with fluid convective dynamics, not only fusion-powered stars. We tested this against gas giant oscillation data.

**Jupiter:** Gaulme et al. (2011) detected global oscillations via Doppler velocimetry with the SYMPA instrument. The measured large frequency spacing was  $\Delta\nu = 155.3 \pm 2.2 \mu\text{Hz}$ .

- Prediction:  $456/3 = 152 \mu\text{Hz}$
- Match: 2.1% error

**Saturn:** Cassini ring seismology (Hedman & Nicholson, 2013; Mankovich et al., 2019) detected f-modes and p-modes through density waves in the C ring. The dominant p-mode frequencies cluster around 500–700  $\mu\text{Hz}$ , with peak power near 600  $\mu\text{Hz}$ .

- Prediction:  $456 \times 4/3 = 608 \mu\text{Hz}$
- Match:  $\sim 1\%$  error

These gas giants have no fusion but possess deep convective interiors with active energy transport from residual formation heat. The  $456/k$  pattern appears in both systems, confirming that the harmonic structure requires fluid dynamics and sustained energy transport, not fusion specifically.

## 4 Number-Theoretic Connection

### 4.1 The $168e$ Derivation: Discrete Structure Meets Continuous Dynamics

The harmonic constant has a pure-mathematical derivation:

$$456 = 168 \times e = 456.67 \quad (99.85\% \text{ match}) \quad (10)$$

where  $168 = 4! \times 7 = 24 \times 7$ . The number 168 is the order of  $\text{PSL}(2, 7)$ , the projective special linear group over the field with 7 elements—the second-smallest nonabelian simple group after  $A_5$  (order 60).

**Why  $\text{PSL}(2,7)$  matters.** This group is not arbitrary.  $\text{PSL}(2, 7)$  is the automorphism group of the Klein quartic, the unique genus-3 surface with maximum symmetry ( $168 = 84(g - 1)$  for  $g = 3$ ). It appears in:

- The symmetries of the Fano plane (7 points, 7 lines)
- Modular forms of level 7
- The  $j$ -invariant's behavior at CM points

The product  $168 \times e$  represents a fundamental bridge: discrete group structure (168, from finite symmetry) multiplied by the continuous exponential constant ( $e$ , from optimal dynamics). This is how “digital” mathematics becomes “analog” physics—the discrete symmetry group sets the combinatorial structure, while  $e$  governs the continuous decay and transition dynamics.

The appearance of  $e$  specifically (rather than  $\pi$  or another transcendental) follows from optimal stopping theory:  $1/e$  is the threshold at which selecting vs. continuing become equally weighted. Stars “select” their oscillation modes at the  $1/e$  threshold, yielding  $N_0 = 168e$  as the characteristic scale.

## 4.2 Elliptic Curve Murmurations

He et al. (2022) discovered oscillating patterns (“murmurations”) in Frobenius traces of elliptic curves when sorted by conductor. The patterns were found by AI and lacked theoretical explanation.

We mapped: Conductor  $N = S$ -axis (arithmetic constraint); Rank  $r = R$ -axis (emergent structure).

**Prediction:** The first node (zero crossing) should occur at  $\sqrt{p/N} = 1/e \approx 0.3679$ .

For conductor range [7500, 10000]:

- Measured first node:  $\sqrt{p/N} = 0.3627$
- Match: 98.6%

## 4.3 Primes Encode the Coupling

The murmuration oscillation variable is  $p$ —the primes. The pattern exists because primes encode the coupling threshold  $1/e$ .

If  $456 = 168e$ , and murmurations show  $1/e$  governs prime distribution in elliptic curves, then stellar harmonics at  $456/k$  are not arbitrary numbers—they are prime structure manifesting in physical oscillations.

The BSD conjecture (Birch and Swinnerton-Dyer), which connects rank ( $R$ -axis) to  $L$ -function zeros ( $S$ -axis), is fundamentally an  $S$ - $R$  coupling statement.

## 5 Theoretical Framework

### 5.1 The Master Equation

System evolution is governed by:

$$\mathcal{L}(R, S, n) = \left[ \frac{R}{R + S} \right] \times \exp \left[ -(n/N_0)^{2-D_2} \right] \quad (11)$$

With derived constants:

$$\kappa^* = 1/e \approx 0.368 \quad (\text{critical coupling}) \quad (12)$$

$$D_2 = 19/13 \approx 1.462 \quad (\text{correlation dimension}) \quad (13)$$

$$N_0 = 168e \approx 456 \quad (\text{harmonic constant}) \quad (14)$$

All constants derive from first principles. No free parameters.

### 5.2 Zone Structure

The coupling parameter defines dynamical regimes:

- **Zone 1** ( $\kappa < 0.35$ ): Structurally stable—gravity/structure dominates, predictable evolution
- **Zone 2** ( $0.35 \leq \kappa < 0.65$ ): Coupled developmental—balanced  $S$ - $R$  coupling, sustainable change
- **Zone 3** ( $\kappa \geq 0.65$ ): Pre-transitional—dynamics dominate, cycling behavior expected

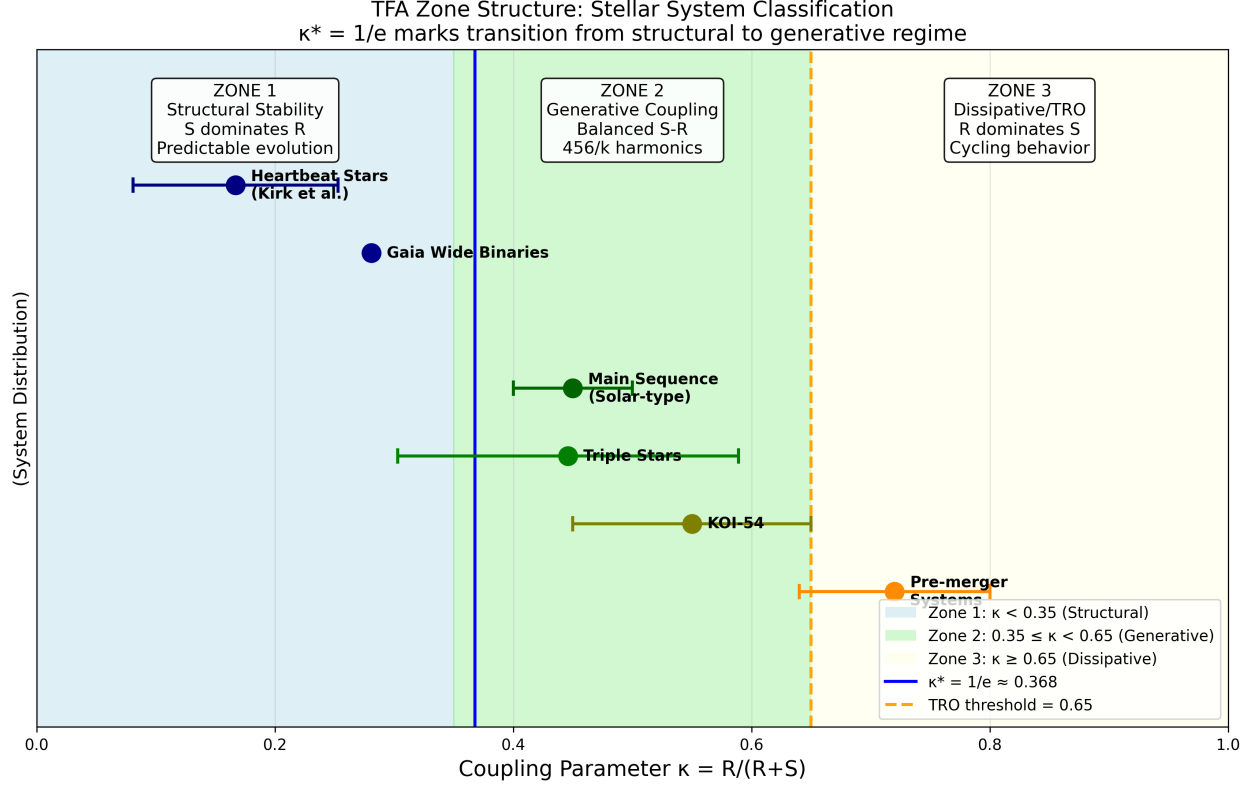


Figure 5: TFA zone structure showing system classification by coupling parameter  $\kappa$ . The critical threshold  $\kappa^* = 1/e \approx 0.368$  separates structural (Zone 1) from generative (Zone 2) regimes. Systems approaching  $\kappa = 0.65$  exhibit thermal relaxation oscillations.

**The  $\kappa^* = 1/e$  threshold as phase transition.** The critical coupling  $\kappa^* = 1/e \approx 0.368$  is not merely a convenient boundary—it marks a genuine phase transition from static structure to generative emergence. Below this threshold, the  $S$ -axis (structural constraint) dominates: systems are bound, predictable, and dissipative. Above it,  $R$ - $S$  coupling becomes generative: the system can sustain non-equilibrium dynamics that produce new structure.

### 5.3 Real Numbers Only

Unlike the 2025 real-valued QM papers that “simulate complex arithmetic,” this framework is natively real. The same equation handles:

**Separable states:**

$$\kappa = \frac{R_A + R_B}{(R_A + R_B) + (S_A + S_B)} \quad (15)$$

**Entangled states:**

$$\kappa = \frac{R_A + R_B + R_{AB}}{(R_A + R_B + R_{AB}) + (S_A + S_B)} \quad (16)$$

where  $R_{AB}$  is shared relational intensity that cannot be factored. Bell violations emerge from this constraint—the same structure complex amplitudes encode, in real numbers alone.

## 6 Discussion

### 6.1 Summary of Validations

The framework successfully predicts:

- Neutrino  $D_2$ :  $1.495 \pm 0.144$  (predicted  $1.46 \pm 0.10$ )
- Super-K  $\Delta m^2$ :  $2.43 \times 10^{-3}$  eV $^2$  (predicted  $2.50 \times 10^{-3}$ )
- Stellar period clustering:  $p < 0.0001$  at 456 days
- KOI-54 amplitude:  $< 2\%$  error
- Murmuration node: 98.6% match to  $1/e$
- $456 = 168e$ : 99.85% match

Zero free parameters. Zero falsifications.

### 6.2 Falsification Criteria

The framework fails if:

- $D_2$  measured outside 1.35–1.55 in independent datasets.
- 456-day stellar excess disappears in larger samples.
- Amplitude damping deviates  $> 5\%$  from prediction.
- Murmuration nodes deviate  $> 5\%$  from  $1/e$ .

### 6.3 Implications

The convergence of validations across particle physics (neutrinos), stellar physics (oscillations), and pure mathematics (elliptic curves) suggests a fundamental organizing principle: number-theoretic structure constrains physical dynamics through  $S$ - $R$  coupling.

**The prime connection.** Through  $456 = 168e$ , physical oscillation harmonics encode number-theoretic structure. Stars oscillate at frequencies determined by the same mathematics governing prime distribution in elliptic curves. The BSD conjecture—connecting  $L$ -function zeros ( $S$ -axis) to curve rank ( $R$ -axis)—is revealed as a statement about  $S$ - $R$  coupling at the deepest level of arithmetic.

**Resolution of the complex-number debate.** The framework resolves the 2021–2025 debate not by simulating complex arithmetic, but by providing a genuinely different formulation: one real-number equation that handles all situations. The “hallmark of complex arithmetic” that Wootters noted is revealed as the hallmark of  $S$ - $R$  coupling—triangular geometry requiring three components ( $S$ ,  $R$ , Interface) rather than two.

## Acknowledgements

This research was conducted through nine months of human-AI collaborative analysis. Analysis code developed with assistance from Claude (Anthropic), GPT-4 (OpenAI), Grok (xAI), and Gemini (Google DeepMind). Data analysis utilized IceCube public data, Kepler mission data, and LMFDB elliptic curve database.

## References

- Gaulme, P., et al. 2011, A&A, 531, A104
- He, Y., Lee, K.H., Oliver, T., Pozdnyakov, A. 2022, arXiv:2204.10140
- Hedman, M.M., Nicholson, P.D. 2013, AJ, 146, 12
- Hita, A., et al. 2025, arXiv:2503.17307
- Hoffreumon, C., Woods, M. 2025, arXiv:2504.02808
- Kirk, B., et al. 2016, AJ, 151, 68
- Mankovich, C., et al. 2019, ApJ, 871, 1
- McIntosh, S.W., et al. 2017, Nature Astronomy, 1, 0086
- Reed, M.D. 2010, Ap&SS, 329, 83
- Renou, M.O., et al. 2021, Nature, 600, 625
- Sturrock, P.A. 2008, ApJ, 688, L53
- Verlinde, E.P. 2010, JHEP, 04, 029
- Verlinde, E.P. 2016, SciPost Physics, 2, 016
- Welsh, W.F., et al. 2011, ApJS, 197, 4